WEATHER RADAR AND LIGHTNING DETECTION SYSTEMS AS COMPLEMENTARY TOOLS FOR HAIL THUNDERSTORM DETECTION

Delobbe Laurent, Crabbé Michel and Hamid Karim
Royal Meteorological Institute of Belgium
Brussels, Belgium

1. INTRODUCTION

Hail is regularly observed in Belgium and is sometimes the cause of severe damage on e.g. crops, greenhouses, roofs and cars. Most severe hail events occur in summer and are associated with intense thunderstorms producing large hail stones. Hail is a very local phenomenon, in time and space, which can not be easily detected with ground observational networks. Remote sensing instruments appear therefore as valuable tools for the real-time detection of hail thunderstorms on a wide spatial coverage and with a relatively fine spatial and time resolution.

The Royal Meteorological Institute of Belgium (RMI) operates a C-band Weather Radar and a SAFIR lightning detection system. A hail detection algorithm based on volumic radar data has been recently implemented at RMI and tested on several reported hail cases. In the present study we investigate the potential contribution of the lightning detection system to the nowcasting of hail thunderstorms. SAFIR data will be compared to radar data for different observed hail cases and we will investigate how SAFIR data can improve the tracking of hail thunderstorms.

The paper is organized as follows. In section 2 we describe SAFIR and radar data and the radar-based hail detection product as well. Comparisons between SAFIR and radar data for different observed hail episodes are shown in section 3. Complementarities between the two observational systems are discussed in section 4. Finally, conclusions are given in section 5.

2. DATA AND PRODUCTS

2.1 SAFIR data

The RMI has been operating a SAFIR (Système d'Alerte Foudre par Interférométrie Radioélectrique) lightning detection system since August 1992. The localization of lightning strikes is performed by triangulation from a network of four antennas in the VHF band (between 108 and 118 MHz). It allows the real time detection of lightning activity with a location accuracy of about 1 km and a time resolution of 100 μs. The antennas are complemented with capacitive electrical antennas which allows discrimination between Intra-Cloud lightning activity (IC) and Cloud-to-Ground lightning activity (CG).

2.2 Radar data and hail product

Since November 2001, the Royal Meteorological Institute of Belgium has been operating a new weather radar in Wideumont, in the South of Belgium, near the borders with France and Luxembourg. The radar is a Gematronik C-band Doppler radar. It performs a standard scan with 5 elevation angles every 5 minutes allowing detection of precipitation up to a maximum range of 240 km. In addition, a volumic scan including 10 elevations is performed every 15 minutes giving a three dimensional view op the reflectivity field in the atmosphere. Volumic radar data allows estimating the vertical extension of thunderstorm cells. This is of great interest for hail detection purpose since the severity of a thunderstorm is strongly related to its vertical extension.

The probability of hail is estimated from radar reflectivity data following the method of Waldvogel et al. (1979) which is operationally used at the Netherlands Royal Meteorological Institute (KNMI). It is based on the difference ΔH (km) between the height of the freezing level and the maximum height at which a reflectivity of 45 dBZ is observed (echotop 45 dBZ). The probability of hail (POH) is calculated as follows:

$$POH = 0.319 + 0.133\,\Delta H$$

This expression has been obtained from a verification study carried out by the KNMI in the summer 2000 (Holleman, 2001). The method of Waldvogel combines an indicator for the presence of a substantial updraft, the height of the strong reflectivity core (45 dBZ),

with that for a large amount of undercooled water and/or ice, the reflectivity core above the freezing level, to detect (developing) hail. The probability of the presence of hail increases with increasing height of this reflectivity core. The method of Waldvogel is currently also being used in the NEXRAD hail detection algorithm (Witt et al., 1998).
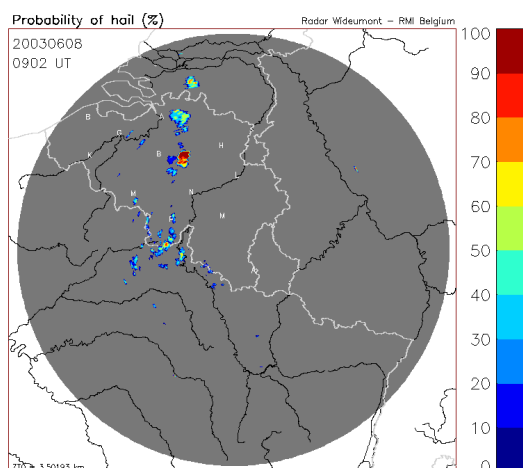

Figure 1: Radar-based hail detection product.

The algorithm was operationally implemented at RMI in 2002. The hail detection product is generated every 15 minutes and gives the probability of hail up to a maximum range of 240 km. Figure 1 shows an example of this product. The hail product was tested on various hail episodes observed in the summer 2002. For 22 cases on 23, a probability of hail at least equal to 50 % was found at less than 10 km from the reported location of hail fall (Delobbe et al., 2003). A few hail cases were reported in the summer 2003 and similar results were obtained.

3. COMPARISON SAFIR-RADAR

For the various reported hail episodes, the SAFIR data have been compared with the radar data in order to get a first idea of the relation between the electrical activity and the occurrence of hail. The comparison has been made for the 23 selected hail cases. The results obtained for a few representative cases are presented in Fig. 2 and 3. The visualization domain is a 60 x 60 km^2 square for both SAFIR and radar probability of hail data. The first figure shows the total lightning activity and the radar-based probability of hail for three different cases (April 19, May 26 and June 4). In the lightning plot, the colours

indicate the time within the total displayed period.

This allows visualizing the displacement of the electrically active area. The first two cases are representative for a quite low thunderstorm intensity. The lightning activity as well as the probability of hail derived from the radar data are low. For the hail episodes of 19 April and 26 May, the vertical extension of the thunderstorm cells was not very high, the size of the hailstones was around 0.5 cm and the height of the freezing level was less than 2 km. These two hail episodes can not be considered as typical hail situations associated with severe thunderstorms but rather as moderately developed convective cells in a relatively cold environment. This is particularly the case for the hail event of 19 April, where the freezing level was as low as 1.3 km. This kind of situation is associated with a relatively low lightning activity compared to severe thunderstorm situations. In contrast, the severe hail episode reported on June 4 is associated with a strong lightning activity and the radar-based probability of hail reaches 100 % in large areas.

The total lightning density, i.e. the number of electrical discharges occurring per square kilometer and per minute is illustrated in Fig. 3. The total density identifies the most active areas in the thunderstorm. The comparisons between the radar and SAFIR data are shown for three cases: June 4, June 14 and July 30. The comparison shows a very good agreement as far as the spatial structure is concerned. Areas with high POH are associated with high electrical activity. The same feature is found for the other hail cases with high electrical activity.

The localization and timing of the lightning activity and the probability of hail have been further analysed for the severe hail case of Lessines (June 4). Hail was produced by a thunderstorm complex moving north-eastward. The time evolution has been split into 4 time intervals of 30 minutes. For each interval, the probability of hail was calculated using the two radar volumic files collected in the given interval. The comparison between the probability of hail and the cloud-to-ground lightning activity for the 4 time intervals is shown in Fig. 4. Again, a very good qualitative agreement between the areas of high POH and the areas of high electrical activity can be observed.

4. COMBINED USE OF SAFIR AND RADAR

Results described in the previous section have shown that the SAFIR system appears as a complementary observational tool with respect to the radar for the real-time detection of severe thunderstorm cells likely to produce hail. A high electrical activity is an indicator for the possible presence of hail.

Besides, lightning detection allows to avoid false alarms related to ground echo's received by the radar. Very strong ground echo's may occur in anomalous propagation (Anaprop) conditions associated with anticyclonic situations, giving rise to false hail detection. Developing thunderstorm cells may be difficult to distinguish from this ground echo's. Lightning detection appears as the easiest way to discriminate between developing thunderstorm cells and ground echo's.

The lightning detection system offers complementarities with the radar for improving the tracking of hail cells. The radar-based hail detection product is generated every 15 minutes which is a relatively long time interval regarding the typical time evolution of a thunderstorm cell. This is of particular importance when automated tracking algorithms are used for extrapolating the position of thunderstorm cells. In many cases, a 15-min interval does not allow a correct cell identification and tracking, especially when splittings and mergings occur. The SAFIR system operated at RMI includes a tracking function allowing to determine the contours of thunderstorm cells, to estimate a velocity vector based on a given integration period and to extrapolate in time providing a short-term forecast of the hazardous areas.

Such warning system combined with the radar-based hail detection algorithm is particularly useful for the tracking of severe hail thunderstorms. Large hail stones are generally produced by supercells or meso convective systems with a very high electrical activity, which facilitates the identification and tracking by a lightning detection system. Severe hail falls associated with a meso-convective system were observed in Belgium on the 8th of June 2003. The storm followed a straight trajectory over a distance of about 150 km. Hailstones with diameters near 5 cm were observed in different places along the trajectory. Figure 5 shows the warning products generated by SAFIR and the radar-based hail detection product as well. The two products are shown at 0915, 0930, 0945 and 1000 UTC. The warning product displays each identified cell in red. For each cell, three shifted dark-coloured areas are displayed and correspond to the expected cell locations after 10, 20 and 30 minutes. The arrow is the velocity vector. It was determined using a 15 min. integration time. The length of the arrow gives the expected displacement over 30 minutes. The comparison with the radar probability of hail shows a very good agreement. In this particular case, the tracking algorithm is able to clearly identify the contours of the thunderstorm and to extrapolate its displacement.

5. CONCLUSIONS

A hail detection algorithm was recently implemented at RMI and tested on various hail episodes observed in Belgium in 2002 and 2003. In the present paper, we discussed the role of a lightning detection system as a complementary tool for hail detection. For the different observed hail cases, lightning data from the SAFIR system were compared with the radar hail data. A very good agreement has been found between the location of the areas of high electrical activity and the areas of high probability of hail. Furthermore, hail cases with larger reported size of hailstones are associated with higher electrical activity.

Further results have shown the utility of the lightning detection system for the tracking of hail thunderstorms. In many weather radar systems, the volumic scan used to generate a hail detection product is only performed every 15 minutes. Lightning data collected at very fast rate allow filling the gap, ensuring a better forecast of hazardous areas. The SAFIR warning function and the radar-based hail detection are currently run separately. In the future, we plan to couple these two systems through a hail warning procedure in which the identification of the cells by the SAFIR tracking algorithm would be restricted to those assigned as hail producers by the radar-based hail detection algorithm.

REFERENCES

Delobbe, L., D. Dehenauw, K. Hamid and J. Neméghaire, 2003. Hail detection using radar observations: case studies in the summer 2002. Scientific report N. 29. Royal Meteorological Institute of Belgium, Brussels.

Holleman, I., 2001. Hail detection using single-polarization radar. Scientific report 2001/01, Royal Netherlands Meteorological Institute (KNMI).

Waldvogel, A., B. Federer, and P. Grimm, 1979: Criteria for the detection of hail cells. J. Appl. Meteor., 18, 1521-1525.

Witt, A., M.D. Eilts, G.J. Stumpf, J.T Johnson, E. D. Mitchell, and K.W. Thomas, 1998. An enhanced hail detection algorithm for the WSR-88D. Wea. and Forecasting, **13**, 286-303.

SAFIR April 19 13.30 to 16.30 UT	Radar-derived POH.
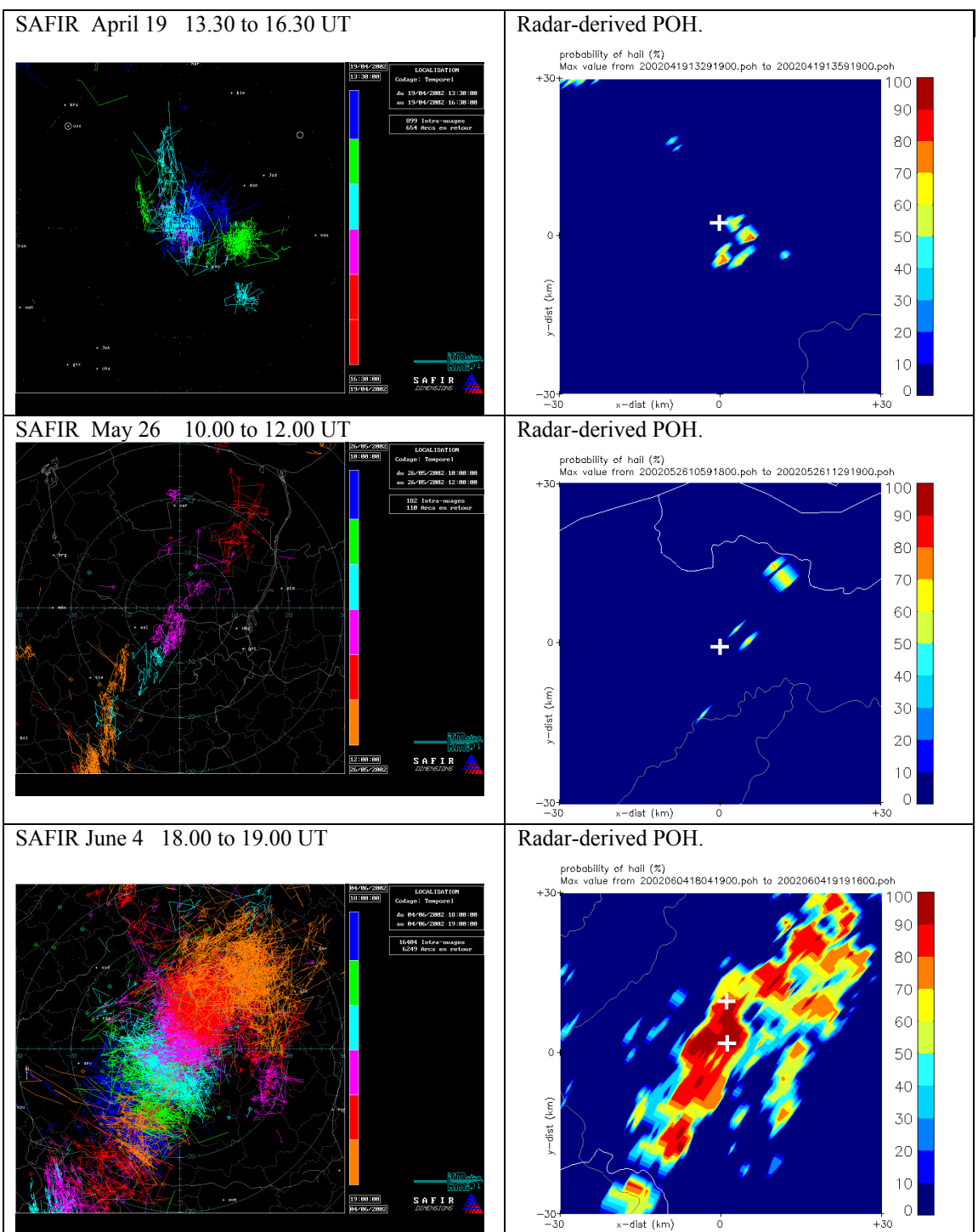
Figure 2: Comparison between lightning activity and radar-derived probability of hail (POH) for hail cases of April 19, May 26 and June 4, 2002.

SAFIR June 4 18.00 to 19.00 UT	Radar-derived POH.
SAFIR June 14 19.00 to 24.00 UT	Radar-derived POH.
SAFIR July 30 13.00 to 17.00 UT	Radar-derived POH.
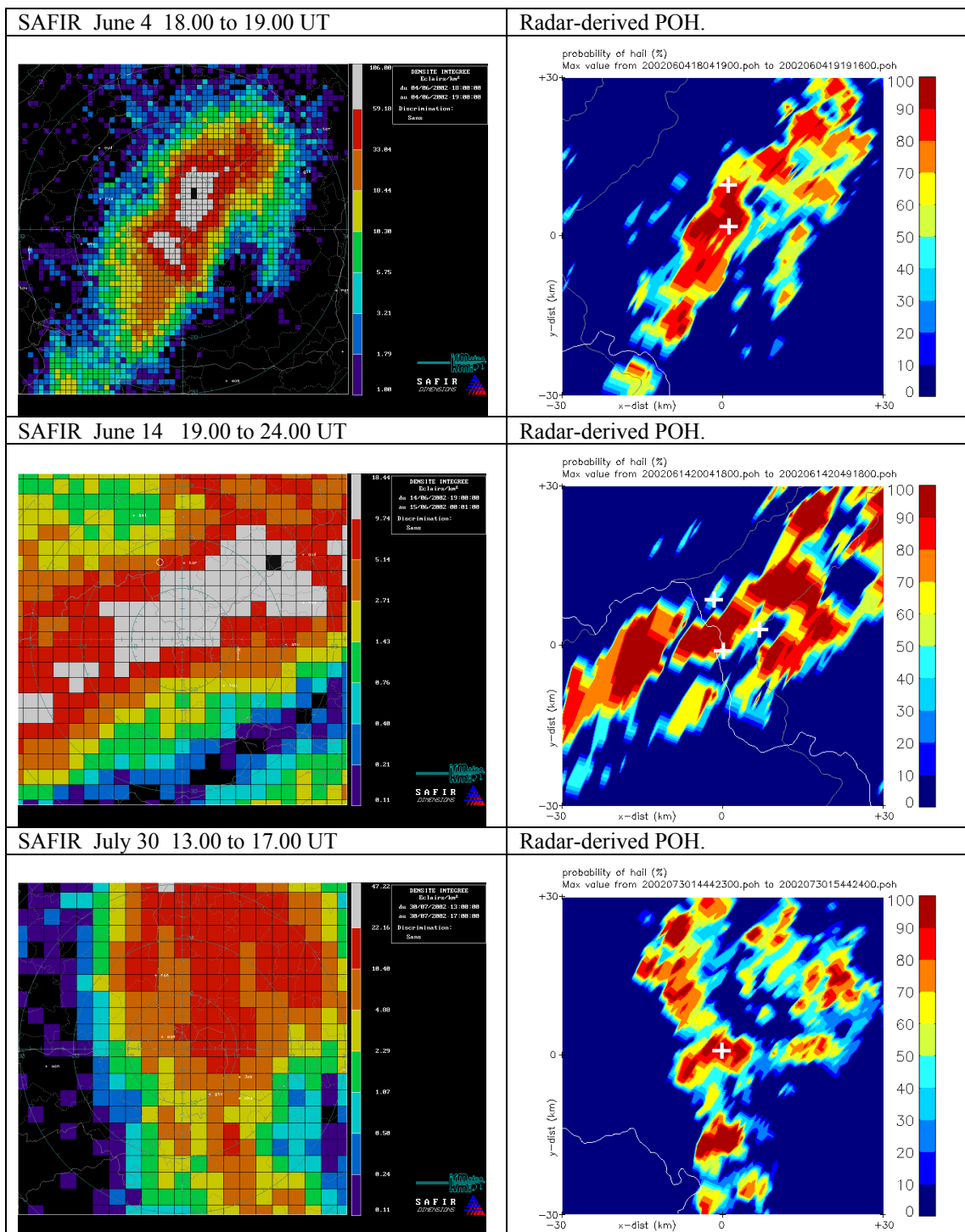
Figure 3: Comparison between lightning density and radar derived
probability of hail (POH) for cases June 4, June 14 and July 30, 2002.

Lightning Localization (SAFIR)   **Probability of Hail (Radar)**

1730
UTC
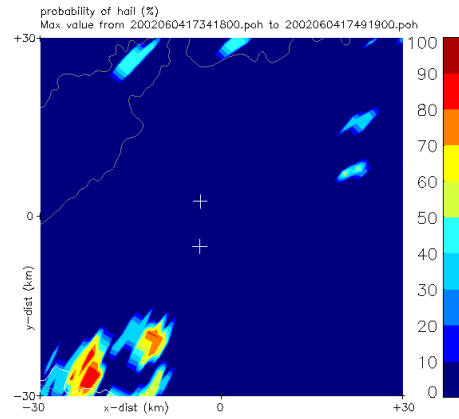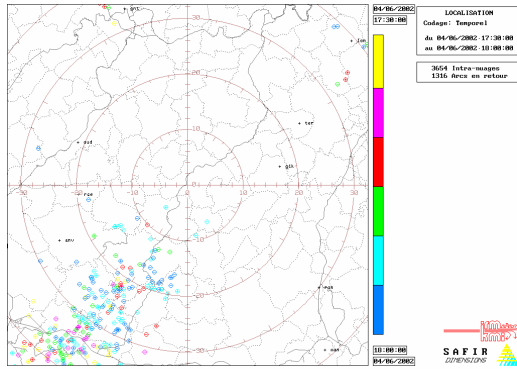
1800
UTC
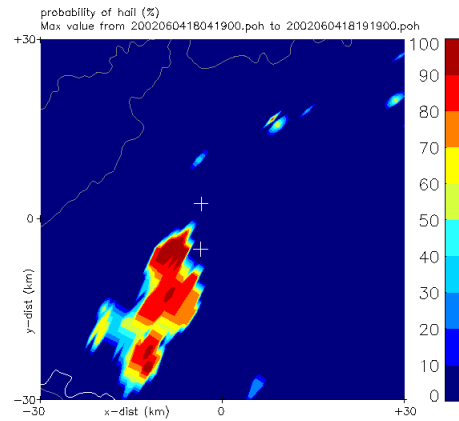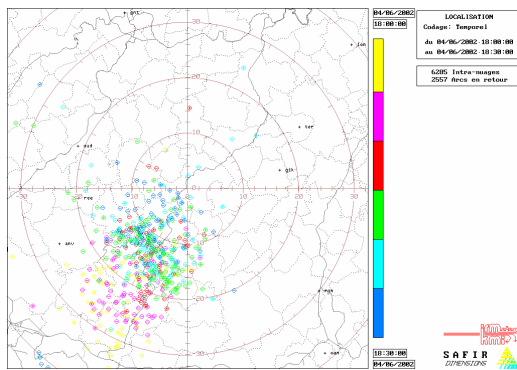
1830
UTC
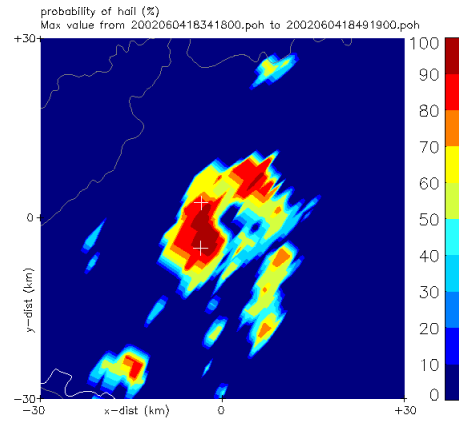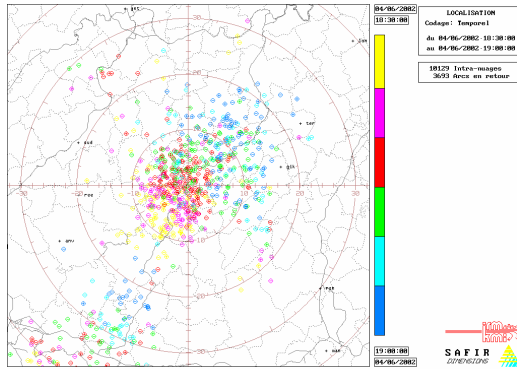
1900
UTC
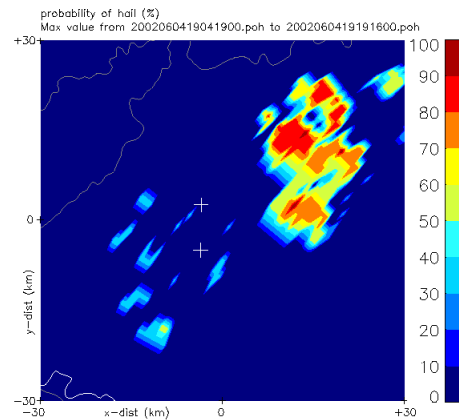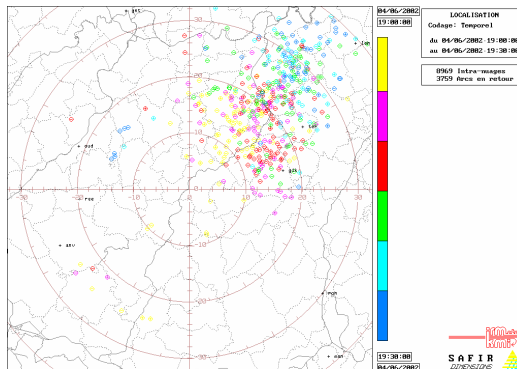
1930
UTC

Figure 4: Comparison between cloud-to-ground lightning activity and radar-derived probability of hail for the hail event of Lessines on June 4, 2002.

**SAFIR WARNING : Expected risk**   **Radar-based Probability of Hail**
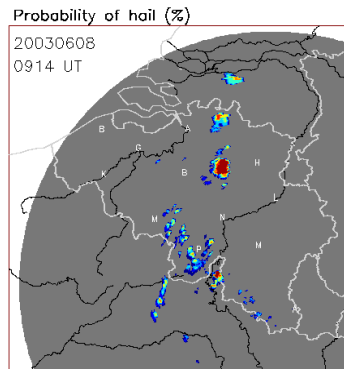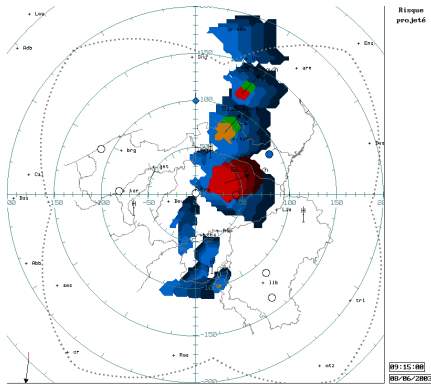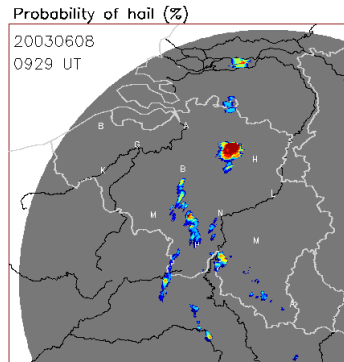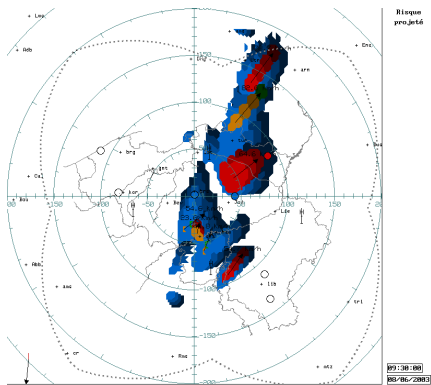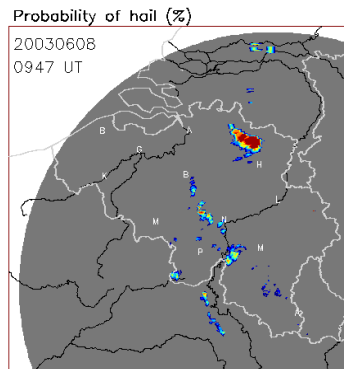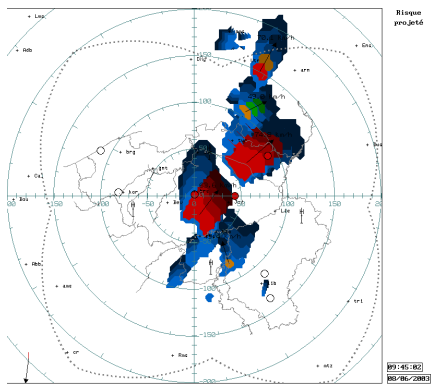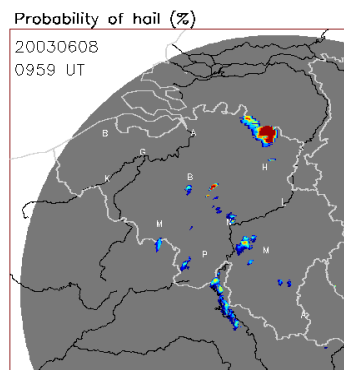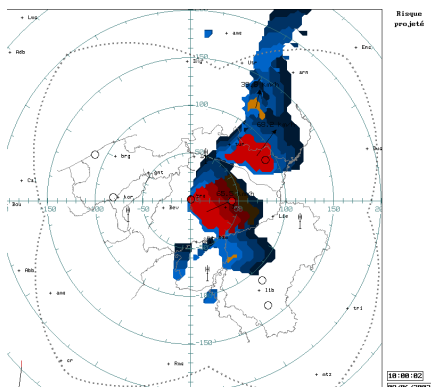
Figure 5: Comparison between SAFIR warning and radar-based hail detection for the hail event of June 8, 2003.